GOSPODARKA SUROWCAMI MINERALNYMI – MINERAL RESOURCES MANAGEMENT

2026 Volume 42 Issue 2 Pages 159–179

DOI: 10.24425/gsm.2026.1429

IRZAL NUR[1], SUFRIADIN SUFRIADIN[2], SRI WIDODO[3],
ANDI A. IBNURUS[4], RAHMAT FEBRIANSYAH[4]

Mineralogical and chemical characteristics of the ion adsorption type REE in West Sulawesi, Indonesia; its exploration and potential utilization implications

Introduction

Rare Earth Elements (REE) are a group of non-ferrous metal elements in the Periodic Table that are categorized as critical material resources. The REE consists of 15 elements of the lanthanide series (plus two other elements with similar chemical characteristics), namely: lanthanum (La), cerium (Ce), praseodimium (Pr), neodymium (Nd), prometheum (Pm), samarium (Sm), europium (Eu), gadolinium (Gd), terbium (Tb), dyprosium (Dy), holmium (Ho), erbium (Er), tulium (Tm), ytterbium (Yb), lutetium (Lu), as well as scandium (Sc) and yttrium (Y) (Balaram et al. 2019; Gunradi et al. 2019).

✉ Corresponding Author: Irzal Nur; e-mail: irzal.nur@eng.unhas.ac.id
[1] Mining Engineering Department, Faculty of Engineering, Hasanuddin University, Indonesia; e-mail: irzal.nur@eng.unhas.ac.id
[2] Mining Engineering Department, Faculty of Engineering, Hasanuddin University, Indonesia; ORCID iD: 0000-0002-6103-3143
[3] Mining Engineering Department, Faculty of Engineering, Hasanuddin University, Indonesia; ORCID iD: 0000-0001-8613-9107
[4] Mining Engineering Department, Faculty of Engineering, Hasanuddin University, Indonesia

Adsorption-type deposits (regolith-hosted REEs) are formed through weathering processes, where REEs are mobile elements that are enriched during the weathering of granite rocks in subtropical areas (Maulana et al. 2016). Adsorption-type REE deposits that develop in the weathering profile of granitoid rocks have been reported in the West Sulawesi province area, with a thickness of up to 1.9 m, with a total REE content (REE+Y+Sc) reaching 373 ppm in the Polewali area, and 336 ppm in the Mamasa area (Alvionita et al. 2023).

Regionally, the stratigraphy of the West Sulawesi region where the research was conducted, composed of from the oldest to the youngest rock units, as follows: Talaya Volcanics (Tmtv) which consists of andesitic-basaltic volcanic breccia, tuff and lava, with intercalations of sandstone and marl, local coal; Adang Volcanics (Tma) which consists of leusite-basaltic tuff, lava and volcanic breccia, mainly micaceous; The Latimojong Formation (Kls) consists of slate, quartzite, phylite, meta quartz sandstone, meta siltstone and marble, locally meta claystone; Intrusive rocks (Tmpi) consisting of granite, granodiorite, rhiolite, diorite, and aplite (Ratman and Atmawinata 1993; Sudjatmiko et al. 1998). Regional geological maps and sampling locations in this study can be seen in Figure 1.

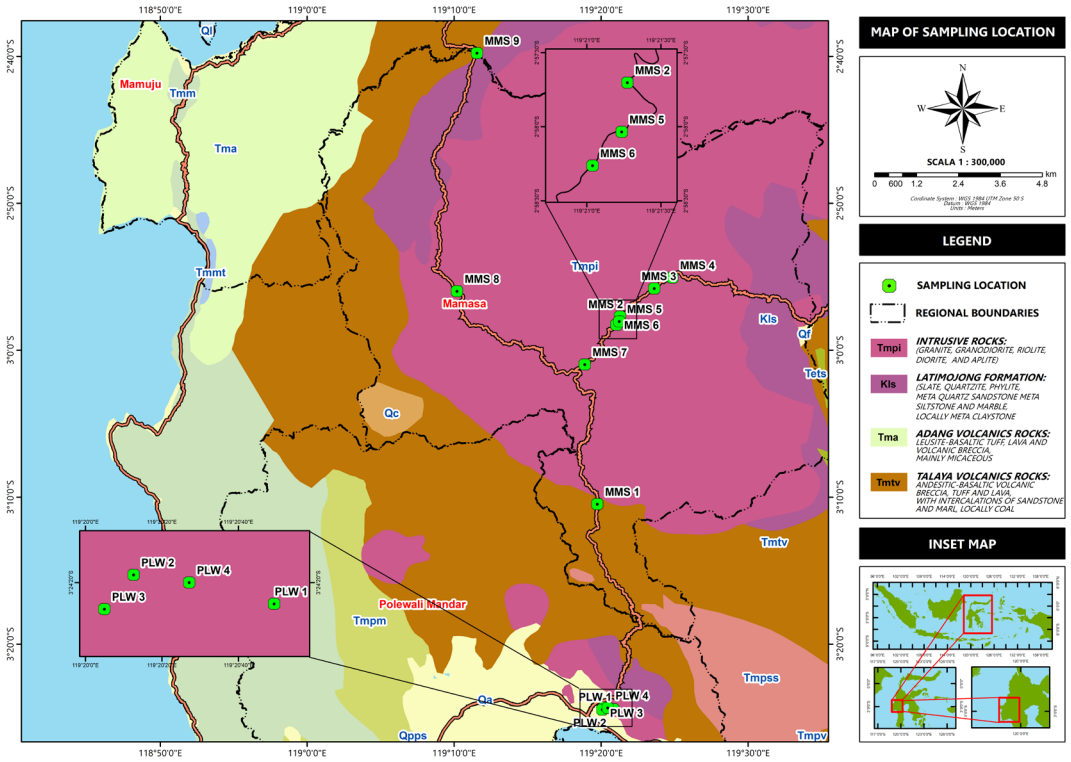

Fig. 1. Regional geological map of West Sulawesi and sampling locations

Rys. 1. Regionalna mapa geologiczna Zachodniego Sulawesi oraz lokalizacje pobrania próbek

This paper describes the results of recent study on the mineralogical and chemical characteristics of the ion adsorption type REE in West Sulawesi, Indonesia; its exploration and potential utilization implications.

1. Methods

In this study, there are three stages of research methods, namely field work, laboratory work, and data processing. Fieldwork includes sampling at locations where laterite deposits from bedrock, granitoid, and volcanic weathering were exposed. In each outcrop, coordinates were taken, and samples were taken in each zone, namely bedrock, saprolite, limonite, and topsoil. Each of these layers, in addition to sampling and observation, also measured the thickness of the zone.

20 samples were collected, of which 16 were categorized as laterite samples while the remaining 4 samples were parent rock. Sample code names were based on sample type, location, and serial number. Generally, two types of samples are used: laterite samples (Horizon O, A, B) and bedrock samples (Horizon C). The weathering profiles were divided into four different layers, i.e., horizon A, B, C, and D, based on the classification by Wu et al. (1990). Location domain codes were PLW for Polewali and MMS for Mamasa. For example, at the MMS 01 station (Figure 2), sampling (Figure 3.A) and thickness measurements (Figure 3.B) were carried out for saprolite (horizon B), limonite (horizon A), and topsoil (horizon O).

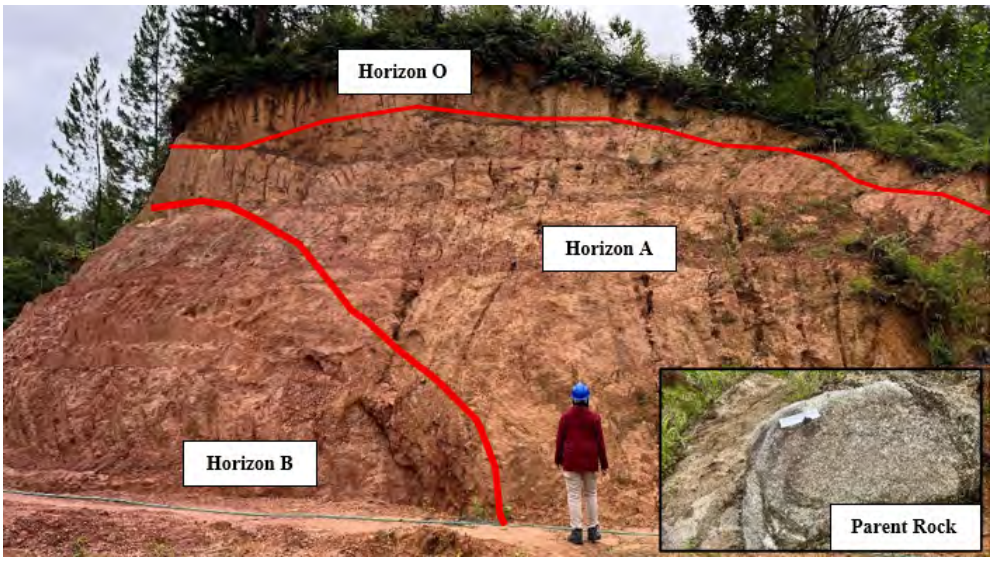

Fig. 2. Granitoid laterite outcrops at MMS Station 01

Rys. 2. Występy laterytu granitoidowego w pobliżu stacji MMS 01

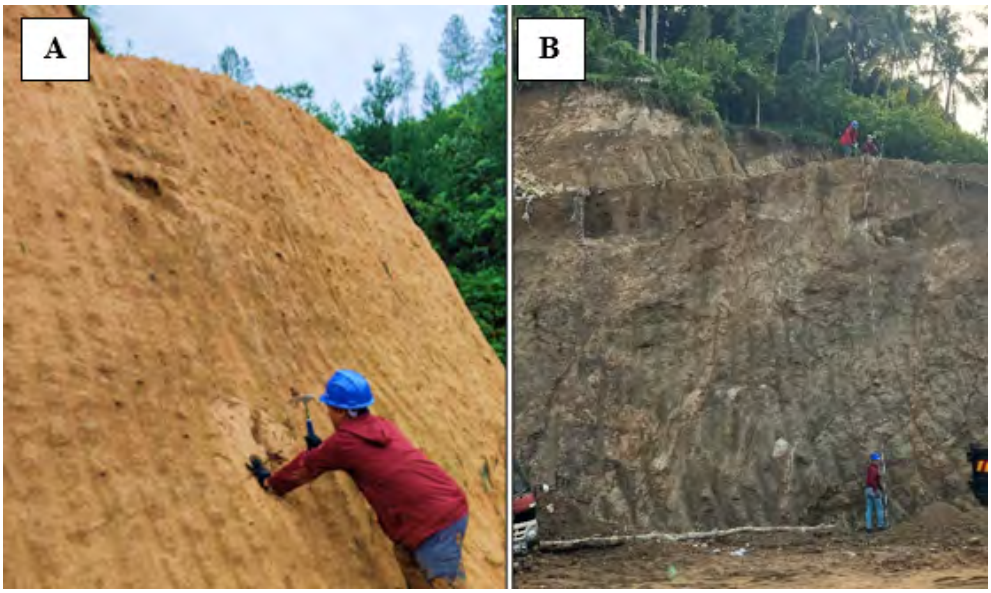

Fig. 3.A. Sampling at MMS Station 01. B. Zone thickness measurement at PLW Station 01

Rys. 3.A. Pobieranie próbek na stacji MMS nr 01. B. Pomiar grubości strefy na stacji PLW nr 01

Before entering the laboratory work stage, sample preparation is first carried out. For rock samples, preparation involves cutting the rock into thin sections, which will then be used for petrographic analysis, and for laterites samples, preparation is carried out in the form of making powder samples that will be used for X-ray diffraction (XRD), X-ray fluorescence (XRF), and inductively coupled plasma mass spectrometry (ICP-MS) analysis.

Petrographic analysis was carried out using a Nikon Eclipse E200 POL-type polarizing microscope to identify mineral sets and bedrock names. XRD analysis was carried out using the Shimadzu Maxima X7000 type XRD instrument to identify the mineral composition of the laterite. The samples were ground to a size of 200 mesh, taken using a spatula, and then ground manually using a mortar and your hands until all the sample grains are smooth and homogeneous (there are no coarse sample grains and the size is the same), then tested with Cu Kα radiation (λ = 1.5406 Å) as an X-ray source. The raw data obtained were in the form of tabular data consisting of 2θ values and intensities, which were then processed by finding the diffraction values. The XRF analysis measured elements including silicon, sodium, magnesium, aluminum, phosphorus, potassium, calcium, titanium, vanadium, chromium, manganese, iron, copper, and zirconium. This XRF analysis was calibrated against a set of 55 geological reference elements, comprising both certified standards (such as those from the International Association of Geoanalysts) and non-certified elements (e.g., from the USGS). Additionally, trace element concentrations were measured using an

Agilent 7500 inductively coupled plasma mass spectrometer (ICP-MS). Petrographic and bulk powder X-ray diffraction (XRD) analysis was conducted at Universitas Hasanuddin (Indonesia). For chemical analysis, trace elements and REE of laterite samples were carried out in Intertek Laboratories in Jakarta by using X-ray fluorescence + LOI (XRFL) and four acids digest with method ICP-MS 4A/OM10 (with a lower detection limit for trace elements) and ICP MS 4A/MS11 (specific to REE) assay methods.

2. Results and discussion

2.1. Bedrock characteristics

In general, 3 types of rocks are recognized: bedrock from REE deposits in West Sulawesi, namely granite in Polewali Mandar Regency, quartz monzonite in Mamasa Regency, and basalt leucite in Mamuju Regency (petrographic naming based on the classification of igneous rocks by Travis 1955). Granite rocks in the Polewali Mandar area show gray to dark gray color, have a phaneritic crystalline texture, and are solid. Under the microscope, a granite rock sample (PLW 02) shows a set of orthoclase minerals, quartz, biotite, hornblende, plagioclase, as well as REE-carrying accessory minerals, namely apatite and zircon (Goodenough et al. 2016; Hui et al. 2025; Zheng et al. 2025) (Figure 4).

Quartz monzonite rock outcrops in the Mamasa area, found with a thickness of more than 7 meters in the Aralle area (MMS 07). Macroscopically, this quartz monzonite rock shows a gray to dark gray color, has a phaneritic crystalline texture, and is solid. Under the microscope, the mineral composition of the two samples (MMS 07 and MMS 08) shows a set of biotite, quartz, orthoclase, plagioclase, opaque minerals, as well as accessory REE-carrying minerals in the form of apatite, monazite, and zircon (Figure 5).

The two types of rocks in the West Sulawesi area that have been described above, namely granite and quartz monzonite, are indeed typical bedrocks from adsorption-type REE deposits. The existence of differences in source batholiths is also thought to influence the intensity of the clay minerals present (Maulana et al. 2016; Alvionita et al. 2023).

2.2. Mineralogy characteristics of type REE adsorption ion deposits

Based on observations in the field, the general profile of adsorption-type REE deposits in the research area (Polewali Mandar and Mamasa) consists of 3 layers, from bottom to top as follows: strong weathered layer or saprolite zone (horizon B), perfect weathered layer or limonite zone (horizon A), and topsoil or humic layer (horizon O) (Figure 2 and Figure 6). This profile is typical in adsorption-type REE deposits (Zhang 1990; Liu and Wang 2016; Alvionita et al. 2023).

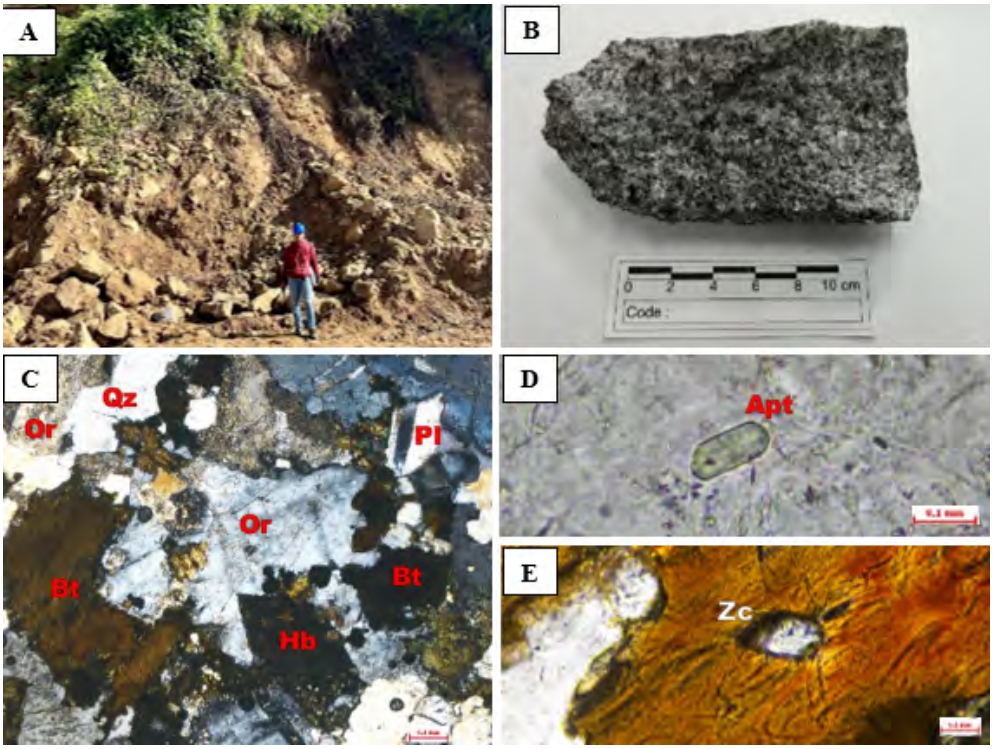

Fig. 4.A. Granite rock outcrop in the Sulewatang area, Polewali Mandar (PLW 02).
B Samples of granite rocks with phaneritic texture (PLW 02). C. Microscopic appearance of granite samples (PLW 02) composed of orthoclase (Or), biotite (Bi), hornblende (Hb), quartz (Qz), plagioclase (Pl).
D. Appearance of accessory minerals of apatite type REE carrier (Apt) on granite samples (PLW 02).
E. Mineral appearance of zircon (Zc) type REE carrier accessories on granite samples (PLW 02)

Rys. 4.A. Odkrywka skały granitowej w rejonie Sulewatang, Polewali Mandar (PLW 02).
B. Próbki skał granitowych o teksturze fanerytowej (PLW 02). C. Wygląd mikroskopowy próbek granitu (PLW 02) złożonych z ortoklazu (Or), biotytu (Bi), hornblendy (Hb), kwarcu (Qz) i plagioklazu (Pl).
D. Wygląd minerałów akcesorycznych typu apatytowego będących nośnikami pierwiastków ziem rzadkich (Apt) w próbkach granitu (PLW 02). E. Wygląd minerałów akcesorycznych typu cyrkonowego (Zc) będących nośnikami pierwiastków ziem rzadkich w próbkach granitu (PLW 02)

In general, laterite deposits on the horizon B in the field show a dominant reddish color, clay-sized, with an average thickness from 8 to 10 meters; horizon A in the field shows a yellowish-red, clay-sized, dominant color with an average thickness from 1 to 5 meters; and horizon O is generally dark brown in color and contains the remains of organic material, with an average thickness of 0,15 meters.

Based on the results of XRD analysis, it was found that the mineral deposits on horizon B are kaolinite, quartz, sanidine, schoepite, halloysite, monazite, dickite, dumontite, waimirite, and montmorillonite for the Mamasa area. As for the Polewali Mandar area, the mineral assemblages found on horizon B are albite, orthoclase, quartz, halloysite, xenotime, zippeite,

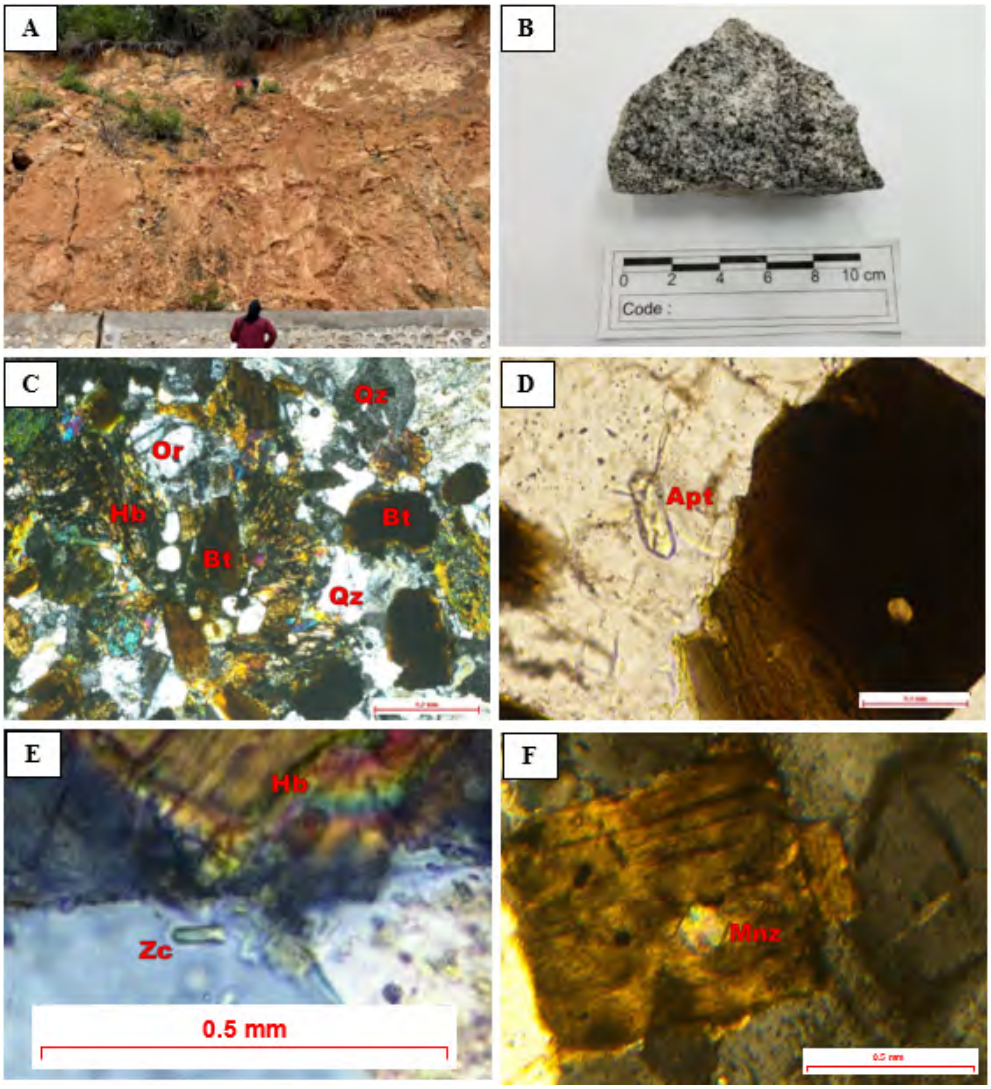

Fig. 5.A. Quartz monzonite rock outcrops in the Aralle area, Mamasa Regency (MMS 07). B. Quartz monzonite rock sample (MMS 08). C. Microscopic appearance of quartz monzonite samples (MMS 07) composed of quartz (Qz), biotite (Bt), hornblende (Hb), and orthoclase (Or). D. Mineral appearance of apatite (Apt) REE carrier accessories on quartz monzonite samples (MMS 07). E. Mineral appearance of zircon-type REE carrier accessories (Zc) in quartz monzonite samples (MMS 07). F. Mineral appearance of monazite (Mnz) type REE carrier accessories in quartz monzonite samples (MMS 08)

Rys. 5.A. Odkrywki skał monzonitu kwarcowego w rejonie Aralle, regencja Mamasa (MMS 07). B. Próbka skały monzonitu kwarcowego (MMS 08). C. Wygląd mikroskopowy próbek monzonitu kwarcowego (MMS 07) złożonych z kwarcu (Qz), biotytu (Bt), hornblendy (Hb) i ortoklazu (Or). D. Wygląd mineralny akcesoriów zawierających pierwiastki ziem rzadkich (REE) typu apatyt (Apt) w próbkach monzonitu kwarcowego (MMS 07). E. Wygląd mineralny akcesoriów zawierających pierwiastki ziem rzadkich (REE) typu cyrkon (Zc) w próbkach monzonitu kwarcowego (MMS 07). F. Wygląd mineralny akcesoriów zawierających pierwiastki ziem rzadkich (REE) typu monacyt (Mnz) w próbkach monzonitu kwarcowego (MMS 08)

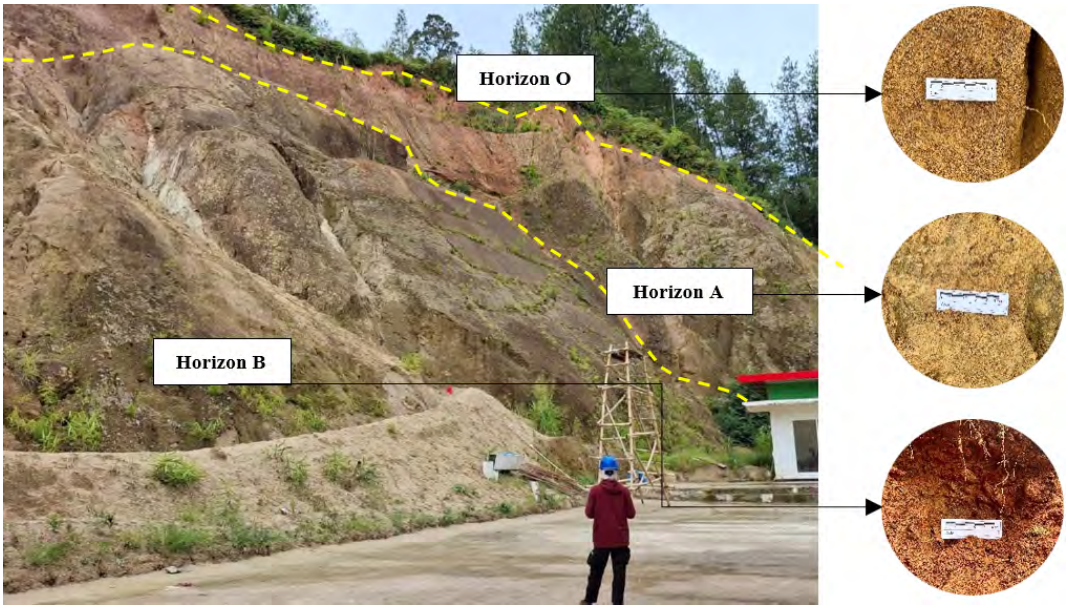

Fig. 6. REE sediment outcrop at Mamasa (MMS 03)

Rys. 6. Występ osadów zawierających pierwiastki ziem rzadkich w Mamasie (MMS 03)

umohoite, and dumontite. On the Mamasa region's A horizon, a mineral assemblage of quartz, muscovite, sanidine, illite, kaolinite, schoepite, and xenotime was found. Meanwhile, on horizon A in the Polewali Mandar area, albit, quartz, halloysite, vermiculite, and xenotime minerals were found.

The identification of REE-carrying minerals in the three laterite layers on the XRD diffractogram was found in samples numbers MMS 03, MMS 04, MMS 07, MMS 08, PLW 01, PLW 03, and PLW 04, namely monazite ($(Ce,La,Nd,Th)PO_4$), xenotime (YPO_4), cozoite ($Nd(CO_3)(OH)$), and waimirite (YF_3). Radioactive minerals were also found in the samples MMS 03, MMS 04, MMS 07, PLW 01, PLW 03, and PLW 04, namely schoepite ($((UO_2)_8O_2(OH)_{12} \cdot 12(H_2O)$), fourmarierite ($((Pb(UO_2)_4O_3(OH)_4 \cdot 4H_2O)$, dumontite ($Pb_2[(UO_2)_3O_2[(PO_4)_2] \cdot 5H_2O$), and zippeite ($K_4(UO_2)_6(SO_4)_3(OH)_{10} \cdot 4(H_2O)$). REE-bearing minerals and radioactive elements are typically present in adsorption-type REE deposits (Goodenough et al. 2016; Hui et al. 2025; Zheng et al. 2025) (Figure 7).

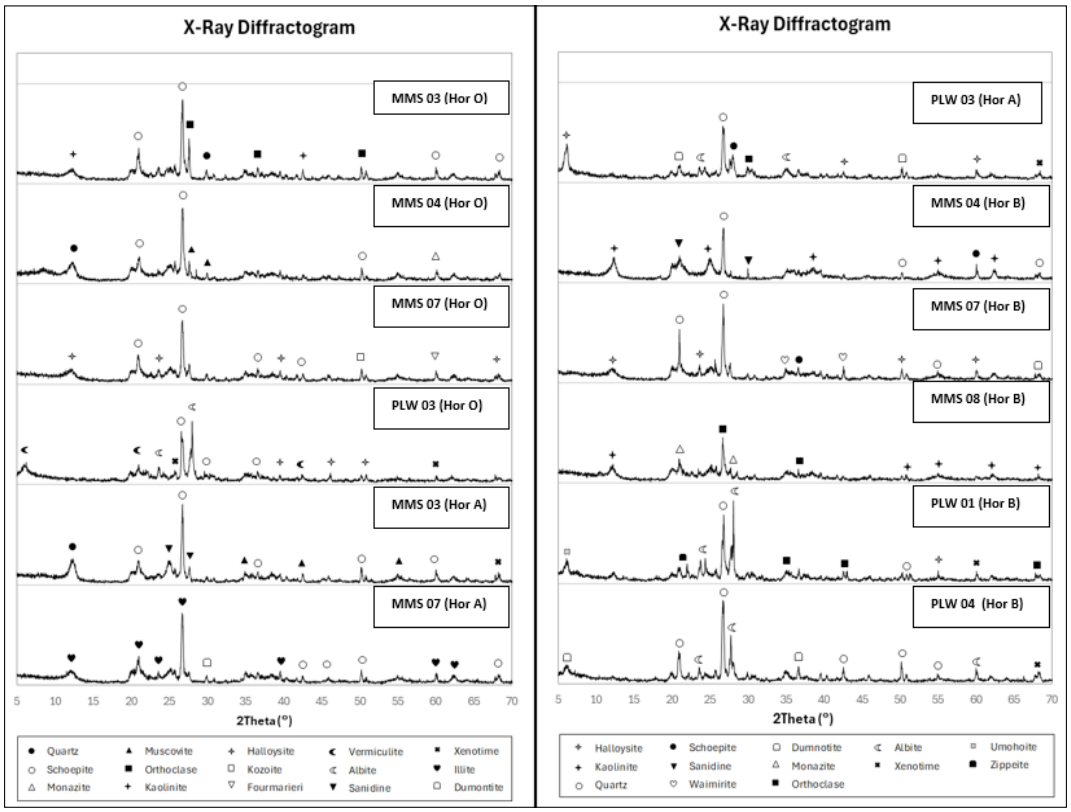

Fig. 7. XRD results of laterites from weathered quartz granite and monzonite of Mamasa and Polewali Mandar

Rys. 7. Wyniki analizy dyfrakcji rentgenowskiej (XRD) laterytów pochodzących ze zwietrzałego granitu kwarcowego i monzonitu z Mamasy i Polewali Mandar

2.3. Chemical characteristics of ion precipitation adsorption type REE

2.3.1. Degree of weathering

The geochemical composition of the major elements can visualize changes in the chemical composition of the granitoid weathering (Figure 8). The high level of chemical weathering is in line with the increase in the value of the Chemical Index of Weathering (CIW), indicating that the presence of clay will be more dominant in granite weathered soil samples. The percentage of CIW values is determined (Equation 1) by the content of Al_2O_3, CaO, and Na_2O, where Al_2O_3 is used as an immobile component, while CaO and Na_2O are mobile elements because they are easily covered during weathering. This index does not contain K_2O (potassium) because it can be covered or accumulated in residues during

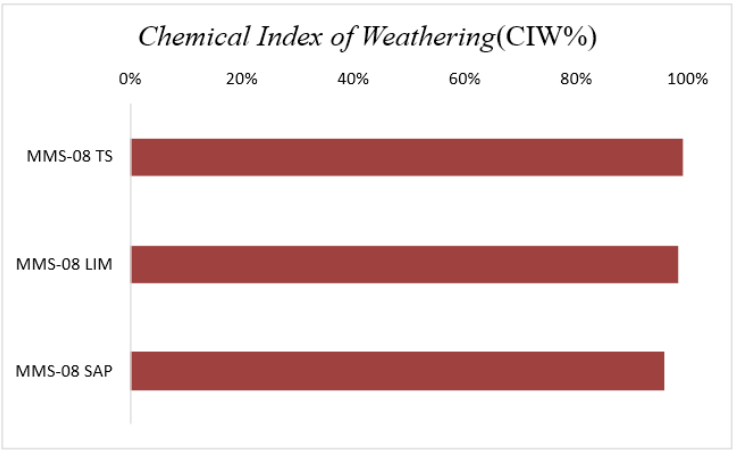

Fig. 8. Chemical Index of Weathering in Mamasa samples

Rys. 8. Wskaźnik chemiczny wietrzenia próbek z Mamasy

weathering (Harnois 1988). In the granitoid weathering sample in Mamasa, the CIW value ranged from 96–98%, this was due to the presence of weathered clay minerals as alumino silicate minerals carrying Al, while the elements Ca and Na, as comparators, had a relatively smaller value because they underwent a washing process.

$$\%CIW = Al_2O_3 / [Al_2O_3 + Na_2O + CaO] \quad (1)$$

In the granitoid weathering sample in Mamasa, the CIW value ranged from 96–98%, this was due to the presence of weathered clay minerals as alumino silicate minerals carrying Al, while the elements Ca and Na, as comparators, had a relatively smaller value because they underwent a washing process. The higher the degree of weathering, which is directly proportional to the presence of clay minerals in the weathered profile, the more REE will possibly be bound by these clay minerals.

2.3.2. REE enrichment pattern on the weathering profile

The weathering profile at Mamasa shows vertical variation in which the total REE increases from horizon B to horizon A and decreases again on horizon O. LREE enrichment on horizon A is also supported by an increase in Ce/La and Ce/REE and elements Th and U (Figure 9) from horizon B to horizon A and decreases again on horizon O. This suggests that REE enrichment occurs on horizon A.

The enrichment of REEs that tend to be enriched in weathered zones containing clay minerals such as kaolinite and halloysite is due to the fact that kaolinite (or halloysite) has

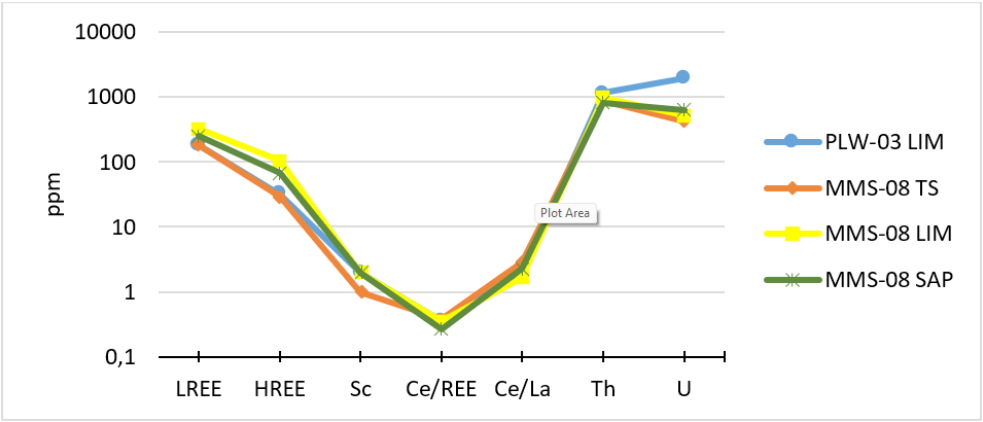

Fig. 9. Variations in REE content in Polewali and Mamasa samples

Rys. 9. Różnice w zawartości pierwiastków ziem rzadkich w próbkach z Polewali i Mamasy

two types of cation exchange, resulting from the substitution of isomorphic Al^{3+} for Si^{4+} (permanent charge) and basal surface (variable charge). REE^{3+} ions are most likely adsorbed on the surface of silica and alumina in clays as $REE(OH)^{2+}$ in acidic solutions (Kosmulski 1997; Marmier et al. 1997; Piasecki et al. 2008).

In general, REE enriched by clay minerals is more predominantly rich in HREE elements than LREE elements (Sanematsu et al. 2016), but if observed, the REE enrichment pattern in this study will show a high LREE/HREE or a greater amount of LREE than HREE. Several factors that cause the enrichment of LREE compared to HREE are caused by minerals related to the mica group, as evidenced by the discovery of biotite through petrographic observations. Biotite binds REEs primarily through coupled ionic substitution in its octahedral layer, where REE^{3+} replaces Fe^{2+}/Mg^{2+}, with charge balance achieved by simultaneous substitutions (like Al^{3+} for Si^{4+}). This process is favored by biotite's specific chemistry (high iron, halogen content) and occurs efficiently in specific geological settings such as granites and hydrothermal systems. While biotite is rarely the primary ore mineral for REEs (that role goes to monazite, bastnasite, etc.), it is an important accessory host that influences the overall distribution and behavior of REEs in rock systems. The existence of LREE enrichment can be related to slab material that is formed during the subduction process and carried to the surface (Kamber et al. 2002; Hakim et al. 2022). In addition, the enrichment of LREE compared to HREE is also caused by the influence of Fe-Mn elements which have the ability to substitute with LREE compared to HREE (Hakim et al. 2022).

Tropical regions, with their pronounced dry and rainy seasons, experience significant groundwater fluctuation. This variability influences the precise location within the profile where REEs become concentrated. Typically, the profile develops an upper zone leached

of REEs and a lower accumulation zone rich in ion-exchangeable REEs. This weathering process also causes geochemical fractionation. Cerium (Ce) often behaves differently, rarely being scavenged from the leached zone, leading to a separation from other REEs. Furthermore, light REEs (LREEs) and heavy REEs plus yttrium (HREEs+Y) can fractionate from each other during the formation of secondary minerals (Sanematsu et al. 2013).

REE-enriched weathering profile with partial ion-adsorption characteristics will show different Ce anomalies. A positive Ce anomaly occurs in the REE leached zone, and a negative Ce anomaly occurs in the accumulation zone of the REE. The relocation zone will be above the REE accumulation zone. The REE concentration in Mamasa shows a positive anomaly of Ce on horizons O and B, which indicates that horizons O and B are the relocation zone, while horizon A shows a negative anomaly of Ce, which indicates an accumulation zone. The highest REE concentrations are also found on horizon A, and the lowest are on horizon O (Kamber et al. 2002; Sanematsu 2016).

2.4. Exploration and potential utilization implications

The abundance of REE (REE+Y+Sc) in Polewali was 226.26 ppm in PLW-03 samples taken from granitoid rock weathering with an LREE of 183.43 ppm and an HREE of 31.8 ppm. Meanwhile, the total REE+Y+Sc in the weathering profile in Mamasa was 228.58 taken in the MMS-08 TS sample on horizon O, in the MMS-08 LIM sample taken on horizon A of 453.37 ppm, and the MMS-08 SAP sample taken on horizon B was 335.6 ppm, with LREE content ranging from 184–330 ppm and HREE ranging from 30–104 ppm (Table 1 and Figure 10).

Table 1. Major elements, trace elements, and rare earth elements in granitoid profiles in Polewali and Mamasa

Tabela 1. Pierwiastki główne, śladowe i ziem rzadkich w profilach granitoidów w Polewali i Mamasie

Sample	Det limit	PLW-03 LIM	MMS-08 TS	MMS-08 LIM	MMS-08 SAP
Major Elements (wt%)					
SiO_2	0.01	66.09	59.85	60.83	62.11
TiO_2	0.01	0.50	0.76	0.76	0.71
Fe_2O_3	0.01	5.49	6.10	6.37	6.52
Al_2O_3	0.01	14.91	17.73	18.92	17.23
MnO	0.01	0.29	0.02	0.09	0.14
MgO	0.01	1.43	1.06	1.71	1.90
CaO	0.01	0.84	0.06	0.11	0.41

Sample	Det limit	PLW-03 LIM	MMS-08 TS	MMS-08 LIM	MMS-08 SAP
K_2O	0.01	4.79	1.42	4.01	4.89
Na_2O	0.01	2.10	0.09	0.23	0.34
P_2O_5	0.002	0.261	0.089	0.062	0.046
Cr_2O_3	0.01	0.05	0.07	0.09	0.05
Total		96.75	87.25	93.18	94.3
Trace elements (ppm)					
Al	50	74,400	90,600	97,900	86,400
Ca	50	5,570	320	700	2,680
Cr	5	268	374	303	273
Cu	1	23	9	22	67
Fe%	0.01	3.83	4.25	4.45	4.42
K	20	38,800	10,600	32,800	38,700
Mg	20	7,820	5,880	9,860	10,500
Mn	1	1,970	162	609	918
Na	20	15,000	610	1,550	2,270
Ni	1	16	56	67	61
P	50	1,090	370	260	190
S	50	60	220	–	–
Ti	5	2,910	4,220	4,610	4,180
V	1	84	71	83	65
Zn	1	133	42	67	108
Ag	0.1	0.4	0.1	–	–
As	1	1,050	2	2	4
Ba	1	1,300	292	769	974
Be	0.5	2.9	2.1	3.3	2.3
Bi	0.05	1.99	5.05	6.73	11.3
Cd	0.05	0.19	0.06	0.08	0.06
Co	1	12	13	26	23
Cs	0.1	29.5	8	15.7	23.4
Ga	0.1	15.8	21.7	24.6	22.1
Ge	0.1	1.1	1.9	2.2	2.4

Sample	Det limit	PLW-03 LIM	MMS-08 TS	MMS-08 LIM	MMS-08 SAP
Hf	0.1	0.5	0.9	1.1	1
In	0.05	0.05	0.08	0.11	0.12
Li	0.1	31.3	23.2	30	27.7
Mo	0.1	5.6	0.9	0.7	0.6
Nb	0.1	12.9	16.4	17.7	14.8
Pb	1	116	51	309	367
Rb	0.1	239	99.5	261	237
Re	0.05	–	–	–	–
Sb	0.1	25.8	0.4	0.4	0.6
Se	1	–	–	–	–
Sn	0.1	2.9	7.7	8.6	11.9
Sr	0.5	254	26.7	70.5	120
Ta	0.05	0.95	1.42	1.59	1.28
Te	0.1	–	0.3	0.3	0.4
Th	0.05	33.5	25.3	28.1	23.8
Tl	0.02	10.3	0.95	1.87	1.95
U	0.05	15.7	3.31	4.25	5.09
W	0.1	11.8	3.5	2.3	3.6
Zr	0.5	6.3	21.1	21.5	15.6
La	0.1	45.6	36.3	82	55.3
Ce	0.1	88.2	103	137	125
Pr	0.05	9.16	8.39	19.6	12.4
Nd	0.1	33.3	30.1	75.2	47
Sm	0.1	5.9	5.6	14.2	9
Eu	0.1	1.3	0.9	2.5	1.7
Gd	0.1	5	4.4	13.3	8.3
Tb	0.05	0.65	0.64	1.92	1.27
Dy	0.1	3.6	3.9	11.5	7.7
Y	0.1	18	15.4	61.8	39.4
Ho	0.1	0.7	0.7	2.2	1.5
Er	0.1	1.8	2	6.4	4.3

Sample	Det limit	PLW-03 LIM	MMS-08 TS	MMS-08 LIM	MMS-08 SAP
Tm	0.1	0.2	0.3	0.8	0.6
Yb	0.1	1.6	1.7	5.2	3.6
Lu	0.05	0.25	0.25	0.75	0.51
Sc	1	11	15	19	18
LREE		183.46	184.29	330.5	250.4
HREE		31.8	29.29	103.87	67.2
TREE		226.26	228.58	453.37	335.6
Ce/Ce*		1.12	1.18	1.15	1.10
(La/Yb)N		20.44	15.32	11.31	11.02

(–) not detected/below the detection limit.

The adsorption of REEs in weathering rocks depends on the properties of the adsorbed material, pH, and ionic radius (Laveuf and Cornu 2009). Weathered granitoids produce fine-grained products that are capable of cation exchange. The enrichment of ΣREE in the granitoids from Polewali and Mamasa was caused by crystallization of apatite, monazite, and zircon. The REE enrichment of the weathered granitoid crust from Mamasa is higher than that from Polewali; this is likely due to the presence of monazite and xenotime, which carry REE, whereas in Polewali, only apatite and zircon were found.

At room temperature, monazite dissolves far more slowly than apatite, even under acidic conditions (pH 2–6) (Harouiya et al. 2007; Oelkers et al. 2008). Unlike some minerals, monazite maintains a crystalline structure in nature and does not become metamict,

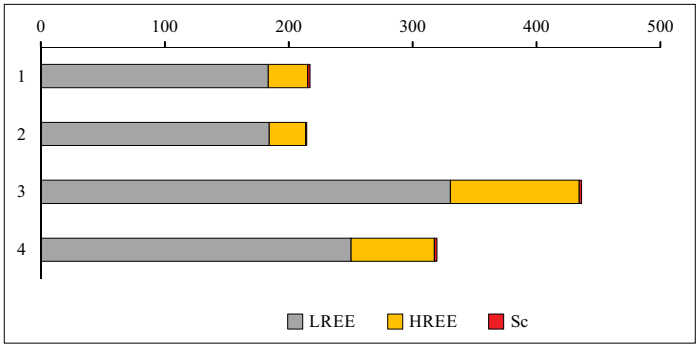

Fig. 10. Bar Chart of the contents of LREE and HREE in West Sulawesi

Rys. 10. Wykres słupkowy przedstawiający zawartość pierwiastków LREE i HREE w Zachodnim Sulawesi

even after significant radiation exposure, because radiation damage is readily repaired over geologic time at low temperatures. Consequently, in weathered granites, fine-grained residual monazite and xenotime are frequently found, while apatite is less common. This resistance to dissolution and weathering explains why monazite is typically concentrated in placer heavy mineral sands and rare earth element deposits (Ravindra Kumar and Sreejith 2010; Sengupta and van Gosen 2016).

Zircon exhibits high resistance to chemical weathering, which explains its frequent presence in ion adsorption ores and its common occurrence in placer sands and sediments (Sanematsu and Kon 2013). Studies have shown that zircon remains more stable under acidic conditions (pH 4–5) than other heavy minerals like apatite, titanite, garnet, and epidote. Although zircon in granites is often found in a metamict (radiation-damaged) state, this damage can be reversed through annealing, even at low temperatures. However, annealing occurs more slowly in zircon than in minerals like monazite (Ewing et al. 2003).

Experiments indicate that zircon dissolves slowly overall, but metamict zircon dissolves more readily than crystalline zircon at temperatures below 150°C. Research on detrital zircon has shown that moderately damaged grains can retain uranium, thorium, and lead, whereas highly damaged grains may release these elements during weathering (Balan et al. 2001). Based on available evidence, the release of rare earth elements (REE) from zircon during weathering appears limited, suggesting zircon contributes little, if at all, to REE in ion adsorption ores.

The distribution of rare earth elements (REEs) in weathered igneous rocks is primarily controlled by the specific REE-bearing minerals present and the intensity of weathering processes (Stille et al. 2009; Yusoff et al. 2013; Sanematsu and Watanabe 2016). A prominent example is observed in southern China, where ion-adsorption ores can contain REY concentrations up to 5.4 times greater than their parent granites, with maximum enrichment typically found in the middle to lower sections of the weathering profile (Yang and Xiao 2011).

The REE levels in Polewali and Mamasa are only able to reach the minimum level that has been successfully mined from the REE mines in China, which is around 336–886 ppm (Longnan), 287–651 ppm (Dingnan), and 311–990 ppm (Quannan) (Sanematsu and Watanabe 2016). However, when compared to the REE levels in granitoid weathering in Indonesia, for example, the REE of adsorption ions on Bangka Island has a level of 70–180 ppm (Syafrizal et al. 2021). The REEs in Polewali and Mamasa are 2 times more than those found on Bangka Island (Figure 11). The results of this study also produced almost the same levels as previous research in West Sulawesi (Alvionita et al. 2023). Despite having lower concentrations of rare earth elements compared to other sources, REE ion-adsorption deposits in lateritic granite are considered promising exploration targets. This is due to their wide geographical spread, economic extraction costs, and the ore's characteristically low levels of thorium and uranium.

REE profiles at the study site will then be normalized to chondrite values (Sun and McDonough 1989). From the results of the analysis, it was found that the LREE > HREE

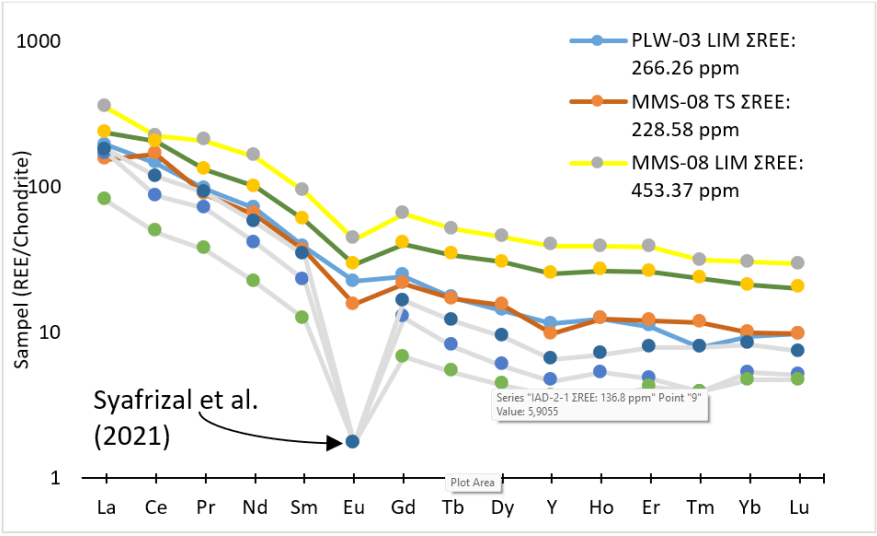

Fig. 11. Normalization of REE against chondrite in West Sulawesi samples. Normalized gray dotted lines from Syafrizal et al. (2021)

Rys. 11. Normalizacja zawartości pierwiastków ziem rzadkich względem chondrytów w próbkach z Zachodniego Sulawesi. Znormalizowane szare linie przerywane pochodzą z pracy Syafrizal i in. (2021)

profile, although the price of HREE is higher than that of LREE because the number is much smaller (Binnemans 2014), but LREE can be used in the manufacture of magnets, electric vehicles, catalysts, metal alloys, cancer treatment, and batteries (Goodenough et al. 2018).

Conclusions

This study characterizes the ion adsorption-type rare earth element (REE) deposits in West Sulawesi, Indonesia, which are derived from the weathering of local granitoid bedrock, specifically granite in Polewali Mandar and quartz monzonite in Mamasa. The weathering profile consists of four distinct layers (bedrock, saprolite, limonite, and topsoil), with mineralogical analysis (XRD) revealing the presence of key REE-bearing minerals such as monazite, xenotime, and zircon, alongside radioactive minerals. Chemically, a high Chemical Index of Weathering (CIW of 96–98%) indicates intense weathering, facilitating REE enrichment, particularly in the limonite (Horizon A), where Light REE (LREE) enrichment is more pronounced than Heavy REE (HREE). This LREE dominance is linked to factors like biotite presence and Fe-Mn element influence. Total REE concentrations (REE+Y+Sc) in the deposits (e.g., up to 453.37 ppm in Mamasa) are approximately double those found in comparable deposits on Bangka Island, though they

are at the lower end of economically mined grades in China. Despite this, the LREE-enriched resources hold potential for various applications, including magnets, electric vehicles, and batteries.

The authors would like to express a deepest gratitude to the Minister of Higher Education, Science and Technology, Indonesia, for the financial support through the Basic Research Scheme (Fundamental Basic Research and Cooperative Research Between Higher Education 2025).

The Authors have no conflict of interest to declare.

REFERENCES

Alvionita et al. 2023 – Alvionita, A.F., Syafrizal and Hakim, A.Y.A. 2023. Mineralogy and enrichment of ion-adsorption type REE on weathered granitoid profiles in West Sulawesi: Implications for exploration. *Jurnal GEOSAPTA* 9(2), pp. 95–104, https://doi.org/10.20527/jg.v9i2.15924.

Balan et al. 2001 – Balan, E., Neuville, D.R., Trocellier, P., Fritsch, E., Muller, J.P. and Calas, G. 2001, Metamictization and chemical durability of detrital zircon: *American Mineralogist* 86, pp. 1025–1033, https://doi.org/10.2138/am-2001-0902.

Balaram, V. 2019. Rare earth elements: A review of applications, occurrence, exploration, analysis, recycling, and environmental impact. *Geoscience Frontiers* 10, pp. 1285–1303, https://doi.org/10.1016/j.gsf.2018.12.005.

Binnemans et al. 2013 – Binnemans, K., Jones, P.T., Blanpain, B., Van Gerven, T., Yang, Y., Walton, A. and Buchert, M. 2013. Recycling of rare earths: A critical review. *Journal of Cleaner Production* 51, pp. 1–22, https://doi.org/10.1016/j.jclepro.2012.12.037.

Binnemans et al. 2014 – Binnemans, K., Vander Hoogerstraete, T., Blanpain, B. and Van Gerven, T. 2014. From NdFeB magnets towards the rare-earth oxides: A recycling process consuming only oxalic acid. *RSC Advances* 4, pp. 64099–64111, https://doi.org/10.1039/C4RA15047H.

Ewing et al. 2003 – Ewing, R.C., Meldrum, A., Wang, L., Weber, W.J. and Corrales, L.R. 2003. Radiation effects in zircon, in Hanchar, J.M. and Hoskin, P.W.O., eds., Zir con: Reviews in Mineralogy and Geochemistry, *Mineralogical Society of America* 53(1), pp. 387–425, https://doi.org/10.2113/0530387.

Goodenough et al. 2016 – Goodenough, K.M., Schilling, J., Jonsson, E., Kalving, P., Charles, N., Tuduri, J., Deady, E.A., Sadeghi, M., Schiellerup, H., Muller, A., Bertrand, G., Arvanitidis, N., Eliopoulus, D.G., Shaw, R.A., Thrane, K. and Keulen, N. 2016. Europe's rare earth element resource potential: An overview of REE metallogenetic provinces and their geodynamic setting. *Ore Geology Reviews* 72, pp. 838–856, https://doi.org/10.1016/j.oregeorev.2015.09.019.

Goodenough et al. 2018 – Goodenough, K.M., Wall, F. and Merriman, D. 2018. The rare earth elements: Demand, global resources, and challenges for resourcing future generations. *Natural Resources Research* 27(2), pp. 201–216, https://doi.org/10.1007/s11053-017-9336-5.

Gunradi et al. 2019 – Gunradi, R., Tampubolon, A., Pardiarto, B., Sunuhadi, D.N., Hilman, P.M., Awaludin, M., Sayekti, B., Faisal, R.M., Hatta, H.M., Sulaeman, Heditama, D.M. and Nugraha, R.S. 2019. The potential of rare earth elements in Indonesia *(in Indonesian)*. Center for Mineral, Coal and Geothermal Resources, Bandung, Indonesia.

Hakim et al. 2022 – Hakim, A.Y.A., Anggayana, K., Indriati, T., Sulistijo, B., Syafrizal, Heriawan, M.N. and Widayat, A.H. 2022. Mineralogy and mobility of elements in lithium and REE in the Sidoarjo mud ("Lusi") *(in Indonesian)*. *Jurnal GEOSAPTA* 8(2), pp. 99–107.

Hakim et al. 2022 – Hakim, A.Y.A., Melcher, F., Prochaska, W. and Meisel, T.C. 2022. Magmatic and metamorphic evolution of the Latimojong Metamorphic Complex, Indonesia. *Journal of Asian Earth Sciences* 227, https://doi.org/10.1016/j.jseaes.2022.105095

Harouiya et al. 2007 – Harouiya, N., Chaïrat, C., Köhler, S.J., Gout, R. and Oelkers, E.H. 2007, The dissolution kinetics and apparent solubility of natural apatite in closed reactors at temperatures from 5 to 50°C and pH from 1 to 6: *Chemical Geology* 244, pp. 554–568, https://doi.org/10.1016/j.chemgeo.2007.07.005.

Hoshino et al. 2016 – Hoshino, M., Sanematsu, K. and Watanabe, Y. 2016. *REE mineralogy and resources*. [In:] *Handbook on the Physics and Chemistry of Rare Earths* 49, https://doi.org/10.1016/B978-0-444-63536-8.00003-4.

Hui et al. 2025 – Hui, C., Sun, F., Yang, Y., Bakht, S., Tian, T., Yu, T., Qiao, J., Chen, X., Liu, C. and Zhang, Y. 2025. Geology and genesis of the Early-Devonian Hatuzhongyou REE deposit, NW China: Insights from petrology, geochemistry, and isotopes. *Geoscience Frontiers* 16, https://doi.org/10.1016/j.gsf.2024.102174.

Kamber et al. 2002 – Kamber, B.S., Ewart, A., Collerson, K.D., Bruce, M.C. and McDonald, G.D. 2002. Fluid-mobile trace element constraints on slab melting and implications for Archaean crustal growth. *Contributions to Mineralogy and Petrology* 144(1), pp. 38–56, https://doi.org/10.1007/s00410-002-0391-5.

Kosmulski, M. 1997 Standard enthalpies of adsorption of di- and trivalent cations on alumina. *Journal of Colloid and Interface Science* 192(1), pp. 215–227, https://doi.org/10.1006/jcis.1997.5023.

Laveuf, C. and Cornu, S. 2009. A review on the potentiality of rare earth elements to trace pedogenesis. *Geoderma* 154, https://doi.org/10.1016/j.geoderma.2009.08.016.

Liu et al. 2016 – Liu, R., Wang, R., Lu, X. and Li, J. 2016. Nano-sized rare earth minerals from granite-related weathering-type deposits in southern Jiangxi. *Acta Petrologica et Mineralogica* 35(4), pp. 617–626.

Maulana et al. 2016 – Maulana, A., Watanabe, K. and Yonezu, K. 2016. Petrology and geochemistry of granitoid from South Sulawesi, Indonesia: Implication for rare earth element (REE) occurrences. *International Journal of Engineering and Science Applications* 3, pp. 79–86.

Marmier et al. 1997 – Marmier, N., Dumonceau, J. and Fromage, F. 1997. Surface complexation modeling of Yb(III) sorption and desorption on hematite and alumina. *Journal of Contaminant Hydrology* 26(1–4), pp. 159–167, https://doi.org/10.1016/S0169-7722(96)00051-4[4].

Oelkers et al. 2008 – Oelkers, E.H., Valsami-Jones, E. and Roncal-Herrero, T. 2008, Phosphate mineral reactivity: from global cycles to sustainable development: *Mineral ogical Magazine* 72, pp. 337–340, https://doi.org/10.1180/minmag.2008.072.2.337.

Piasecki, W. and Sverjensky, D.A. 2008. Speciation of adsorbed yttrium and rare earth elements on oxide surfaces. *Geochimica et Cosmochimica Acta* 72(16), pp. 3964–3979, https://doi.org/10.1016/j.gca.2008.05.041.

Ratman, N. and Atmawinata, S. 1993 Geologic map of the Mamuju quadrangles, Sulawesi. Geological Research and Development Centre, Bandung, Indonesia.

Ravindra Kumar, G.R. and Sreejith, C. 2010, Relationship between heavy mineral placer deposits and hinterland rocks of southern Kerala: A new approach for source-to-sink link from the chemistry of garnets. *Indian Journal of Geo-Marine Sciences* 39(4), pp. 562–571.

Sanematsu, K. and Kon, Y. 2013, Geochemical characteristics determined by multiple extraction from ion-adsorption type REE ores in Dingnan County of Jiangxi Province, South China: *Bulletin of the Geological Survey of Japan* 64, pp. 313–330, https://doi.org/10.9836/bullgsj.64.313.

Sanematsu, K. and Watanabe, Y. 2016. Characteristics and genesis of ion-adsorption type rare earth element deposits. *Reviews in Economic Geology* 18, pp. 55–79, https://doi.org/10.5382/Rev.18.03.

Sanematsu et al. 2013 – Sanematsu, K., Kon, Y., Imai, A., Watanabe, K. and Watanabe Y. 2013, Geo chemical and mineralogical characteristics of ion-adsorption type REE min eralization in Phuket, Thailand: *Mineralium Deposita* 48, pp. 437–451, https://doi.org/10.1007/s00126-012-0440-5.

Sengupta, D. and Van Gosen, B.S. 2016, Placer-type rare earth element deposits: *Reviews in Economic Geology* 18, pp. 81–100, https://doi.org/10.1130/abs/2016AM-279551.

Stille et al. 2009 – Stille, P., Pierret, M. C., Steinmann, M., Chabaux, F., Boutin, R., Aubert, D., Pourcelot, L. and Morvan, G. 2009, Impact of atmospheric deposition, bio geochemical cycling and water-mineral interaction on REE fractionation in acidic surface soils and soil water (the Strengbach case): *Chemical Geology* 264, pp. 173–186.

Sudjatmiko et al. 1998 – Sudjatmiko, S., Sukadana, I.G., Rosana, M.F. and Prasetyadi, C. 1998. Geologi Map of the Mamuju Quadrangles, West Sulawesi. Geological Research and Development Centre, Bandung, Indonesia, https://doi.org/10.1016/j.chemgeo.2009.03.005.

Sun, S.S. and McDonough, W.F. 1989. *Chemical and isotopic systematics of oceanic basalts: Implications for mantle composition and processes*. [In:] Saunders, A.D. and Norry, M.J. (eds), *Magmatism in the Ocean Basins*, Geological Society Special Publication 42, pp. 313–345, https://doi.org/10.1144/GSL.SP.1989.042.01.19.

Syafrizal Hede et al. 2021 – Syafrizal Hede, A.N.H., Hakim, A.Y.A. and Permatasari, M.I. 2021. Identification of the presence of ion-adsorption type rare earth elements in Bangka clay (*in Indonesian*). *Jurnal GEOSAPTA* 7(2), http://dx.doi.org/10.20527/jg.v7i2.10897.

Travis, R.B. 1955. Classification of rocks. *Colorado School of Mines Quarterly* 50(1), pp. 1–98.

Wu, C.Y. and Ishihara, S. 1994. REE geochemistry of the Southern Thailand granites. *Journal of Southeast Asian Earth Sciences* 10(1–2), pp. 81–94, https://doi.org/10.1016/0743-9547(94)90010-8.

Yang, D.H. and Xiao, G.M. 2011. Regional metallogenic regularities of the ion adsorption type of rare-earth deposits in Guangdong Province: *Geology and Resources* 20, pp. 462–468 (*in Chinese with English abstract*), https://doi.org/10.13686/j.cnki.dzyzy.2011.06.005.

Yusoff et al. 2013 – Yusoff, Z.M., Ngwenya, B.T. and Parsons, I. 2013. Mobility and fractionation of REEs during deep weathering of geochemically contrasting granites in a tropical setting, Malaysia. *Chemical Geology* 349, pp. 71–86, https://doi.org/10.1016/j.chemgeo.2013.04.016.

Zhang, Z. 1990. A study on weathering-crust ion-adsorption type rare earth element deposits, South China. *Contributions to Geology and Mineral Resources Research* 5(1), pp. 57–71.

Zhao et al. 2025 – Zhao, X., Li, N., Yu, H., Wang, Y. and Niu, H. 2025. Post-magma hydrothermal activity contributed to the generation of Bachi ion-adsorption REE deposits in South China. *Ore Geology Reviews* 183, https://doi.org/10.1016/j.oregeorev.2025.106678.

MINERALOGICAL AND CHEMICAL CHARACTERISTICS OF THE ION ADSORPTION TYPE REE IN WEST SULAWESI, INDONESIA; ITS EXPLORATION AND POTENTIAL UTILIZATION IMPLICATIONS

Keywords

geochemistry, mineralogy, Rare Earth Elements, ion adsorption clay

Abstract

This study characterizes ion adsorption-type rare earth element (REE) deposits in West Sulawesi, Indonesia, derived from the weathering of local granitoid bedrock. The investigation focuses on granite in Polewali Mandar and quartz monzonite in Mamasa as the primary host rocks. The research integrated fieldwork by systematic sampling of weathering profile zones and laboratory analyses, including petrography, XRD, XRF, and ICP-MS. The weathering profile is typical of ion-adsorption deposits, comprising four distinct layers from bottom to top: bedrock (C), saprolite (B), limonite (A), and topsoil (O). Mineralogical analysis identified key REE-bearing minerals such as monazite, xenotime, and zircon within the weathered layers, alongside associated radioactive minerals. Chemically, a high Chemical Index of Weathering (CIW: 96–98%) confirms intense weathering conditions. Results reveal significant REE enrichment, particularly in the limonit (Horizon A), with total REE+Y+Sc concentrations reaching up to 453.37 ppm in Mamasa. The deposits are characterized by a pronounced enrichment of Light REEs (LREE) over Heavy REEs (HREE), attributed to factors including the presence of biotite and the influence of Fe-Mn elements. While the total REE concentrations are approximately double those found in comparable deposits on Bangka Island (70–180 ppm), they are

at the lower end of economically mined grades in China. Despite this, the LREE-enriched resources from West Sulawesi hold potential for various technological applications, including the manufacture of magnets, electric vehicles, catalysts, and batteries. This study underscores the regional potential of these deposits and provides a foundation for further exploration and utilization assessment.

CHARAKTERYSTYKA MINERALOGICZNA I CHEMICZNA PIERWIASTKÓW ZIEM RZADKICH TYPU ADSORPCYJNEGO W ZACHODNIEJ CZĘŚCI WYSPY SULAWESI W INDONEZJI; IMPLIKACJE DLA POSZUKIWAŃ I POTENCJALNEGO WYKORZYSTANIA

Słowa kluczowe

geochemia, mineralogia, pierwiastki ziem rzadkich, glinki adsorbujące jony

Streszczenie

W niniejszym badaniu scharakteryzowano złoża pierwiastków ziem rzadkich (REE) typu adsorpcji jonowej w zachodniej części wyspy Sulawesi w Indonezji, powstałe w wyniku wietrzenia lokalnego podłoża granitoidowego. Badania skupiają się na granicie w regionie Polewali Mandar oraz monzonicie kwarcowym w regionie Mamasa jako głównych skałach macierzystych. Badania obejmowały prace terenowe polegające na systematycznym pobieraniu próbek z poszczególnych stref profilu wietrzenia oraz analizy laboratoryjne, w tym petrografię, XRD, XRF i ICP-MS. Profil wietrzenia jest typowy dla złóż typu adsorpcji jonowej i składa się z czterech odrębnych warstw od dołu do góry: podłoża skalnego (C), saprolitu (B), limonitu (A) oraz wierzchniej warstwy gleby (O). Analiza mineralogiczna pozwoliła zidentyfikować kluczowe minerały zawierające pierwiastki ziem rzadkich, takie jak monacyt, ksenotym i cyrkon w warstwach zwietrzałych, a także towarzyszące im minerały radioaktywne. Pod względem chemicznym wysoki wskaźnik zwietrzenia (CIW: 96–98%) potwierdza intensywne warunki zwietrzenia. Wyniki wskazują na znaczne wzbogacenie w pierwiastki ziem rzadkich, szczególnie w limonicie (horyzont A), gdzie całkowite stężenie REE+Y+Sc osiąga nawet 453,37 ppm w Mamasie. Złoża charakteryzują się wyraźnym wzbogaceniem w lekkie pierwiastki ziem rzadkich (LREE) w stosunku do ciężkich pierwiastków ziem rzadkich (HREE), co przypisuje się czynnikom takim jak obecność biotytu i wpływ pierwiastków Fe-Mn. Chociaż całkowite stężenia pierwiastków ziem rzadkich są około dwukrotnie wyższe od tych występujących w porównywalnych złożach na wyspie Bangka (70–180 ppm), plasują się one w dolnej granicy ekonomicznie opłacalnych zawartości w Chinach. Mimo to złoża bogate w pierwiastki ziem rzadkich z Zachodnim Sulawesi mają potencjał do wykorzystania w różnych zastosowaniach technologicznych, w tym do produkcji magnesów, pojazdów elektrycznych, katalizatorów i akumulatorów. Niniejsze badanie podkreśla regionalny potencjał tych złóż i stanowi podstawę do dalszych poszukiwań oraz oceny możliwości ich wykorzystania.